Applied Catalysis B: Environmental 110 (2011) 231–237

Contents lists available at SciVerse ScienceDirect

Applied Catalysis B: Environmental

journal homepage: www.elsevier.com/locate/apcatb

VOCs combustion catalysed by platinum supported on manganese octahedral molecular sieves

O. Sanz[a,*], J.J. Delgado[b], P. Navarro[a], G. Arzamendi[c], L.M. Gandía[c], M. Montes[a]

[a] Applied Chemistry Department, University of Basque Country (UPV-EHU), Apdo. 1072, 20080 San Sebastian, Spain
[b] Materials Science Department, Metallurgical Engineering and Inorganic Chemistry, University of Cádiz, E-11510 Puerto Real, Spain
[c] Departamento de Química Aplicada, Edificio de los Acebos, Universidad Pública de Navarra, Campus de Arrosadía s/n, E-31006 Pamplona, Spain

ARTICLE INFO

Article history:
Received 13 May 2011
Received in revised form 5 September 2011
Accepted 9 September 2011
Available online 16 September 2011

Keywords:
Pt-OMS-2
Catalytic VOCs combustion
VOCs mixture
Cryptomelane

ABSTRACT

In this work a manganese oxide in the form of octahedral molecular sieve (OMS-2, also called cryptomelane) has been synthesized and used as catalyst and support for Pt. The catalysts were tested and compared with Pt-Al_2O_3 in the combustion of methyl-ethyl-ketone (MEK), toluene, ethyl acetate and a mixture of toluene and ethyl acetate. Bare OMS-2 was significantly active for the combustion of the oxygenated VOCs and in the case of MEK partial oxidation product was detected at intermediate conversion levels. Platinum on OMS-2 showed high dispersion and improved the activity for toluene oxidation, showing a performance better than that of Pt-Al_2O_3. As for the VOCs mixture, Pt-OMS-2 presented the highest combustion activity due to the coexistence of active sites for the total oxidation of both aromatic and oxygenated VOCs. Competitive adsorption effects were not observed with this catalyst that achieved complete conversion of 1000 mg C/m^3 of VOCs at temperatures below 260 °C (1200 mg C $g_{catalyst}^{-1}$ h^{-1}).

1. Introduction

Volatile organic compounds (VOCs) are an important group of primary atmospheric air pollutants. They are commonly found in the atmosphere in significant quantities in both urban and industrial areas. The significance of the abatement technologies for the removal of VOCs from industrial effluents has increased greatly with the introduction of stringent legislation to control their release to the environment. Various techniques have been proposed, one of these being the heterogeneous catalytic oxidation of VOCs to carbon dioxide and water which is characterized by relatively low operating temperatures, so extremely active catalysts are required.

Within the transition metal oxide catalysts, manganese oxides present very interesting properties as catalyst for VOCs total oxidation because of the multiple different coordination numbers and oxidation states that Mn can adopt, as well as the presence of defects (primarily oxygen vacancies). Of particular importance are the octahedral molecular sieves (OMS-2), also called cryptomelane-type manganese oxides. OMS-2 is a crystalline solid that is found in nature as a porous material [1–3]. The primary porosity corresponds to the tunnel formed by the 2×2 edge sharing [MnO_6] octahedral chains. This 4.6 Å tunnels are occupied by K^+ acting as template that stabilizes the OMS-2 structure. Therefore, this microporosity is not available for adsorption. The OMS-2 structure induces a nanofibrillar form to the solid and the agglomeration of nanofibers forms bunches showing mesopores between the fibers. This structure is responsible for the high surface area and mesoporosity exposed by the OMS-2 solids [4].

The activity of manganese catalysts has been often improved by using different supports, special preparation routes or the addition of transition and noble metals. OMS-2 modified with the incorporation of different dopants, including cerium, zirconium, copper, titanium, nickel, cobalt, silver and platinum, attracts much attention in many catalytic processes [5–12]. The incorporation of various transitions metal ions in the OMS-2 material provides modified surface acid–base and electronic properties on the oxide lattice [13]. The morphology of the doped OMS-2 depends on the preparation method. Wang et al. [11] observed that when the dopant is incorporated during the OMS-2 synthesis, the formed structure had small particles rather than the needle-shape nanocrystal structure, while if the ion was introduced after formation of OMS-2, the structure remained unchanged. It has been found that the introduction of silver to the manganese oxide system strongly increased the activity of the catalyst in the total oxidation of CO [12] and the combustion of VOCs [14]. Pt doped OMS-2 has been investigated for HCOH elimination [11]. The advantage of this material is that Pt forms lattice defects enhancing the mobility of oxygen species and therefore promoting the oxidation activity.

The platinum group metal catalysts have high efficiencies for the complete oxidation of aromatic compounds such as benzene, toluene and xylenes. However, the temperatures required for the oxidation of oxygenated VOCs using platinum group metal are

* Corresponding author.
E-mail address: oihane.sanz@ehu.es (O. Sanz).

0926-3373/$ – see front matter © 2011 Elsevier B.V. All rights reserved.
doi:10.1016/j.apcatb.2011.09.005

usually higher than that over transition metal oxide catalysts [15]. The aim of this work was to prepare a single catalyst composed of manganese and platinum oxide suitable for combustion of aromatics and oxygenates. A OMS-2 manganese oxide was synthesized and taking advantage of its excellent textural properties was used as support for platinum. The catalytic activity was measured for the complete oxidation of MEK, toluene, ethyl acetate and a mixture of toluene and ethyl acetate.

2. Experimental

2.1. Preparation of OMS-2 type oxide

The reflux method proposed by Luo et al. [16] was used to prepare the cryptomelane. Briefly, 11 g of $MnAc_2{\cdot}4H_2O$ (Aldrich) were dissolved in 40 cm^3 of a buffer solution containing 5 ml of glacial acetic acid and 5 g of KAc in 40 cm^3 of deionized distilled water (DDW). To this buffered solution 150 cm^3 of DDW containing 6.5 g of $KMnO_4$ (Aldrich) was added slowly while stirring and further refluxed under continuous stirring for 24 h (pH 4.5). At the end of the synthesis procedure the obtained solid was filtered, washed, dried at 120 °C for 30 min, and finally calcined in air at 500 °C for 2 h.

2.2. Preparation of platinum supported catalyst

The Pt-Al_2O_3 (γ-Al_2O_3 Spheralite 505, Procatalyse; 100–200 μm particle size fraction) and Pt-OMS-2 catalysts were prepared by incipient wetness impregnation with an aqueous solution of $Pt(NH_3)_4(OH)_2$ (Johnson Matthey, Alfa). Concentration was established in order to introduce 1% Pt into the pore volume. After impregnation, the catalysts were dried at 120 °C for 2 h and calcined at 450 °C for 2 h.

2.3. Characterization techniques

X-ray diffraction (XRD) analyses were carried out on a Philips PW 1729-1820 diffractometer. Diffraction patterns were recorded using Cu K_α radiation. The crystal phases were identified using PDF2 database from International Centre for Diffraction Data.

The textual properties were studied by N_2 adsorption measurements at liquid nitrogen temperature using Micromeritics ASAP 2020 equipment. Specific surface area was calculated according to the BET method, external and microporous area using *t*-plot, total pore volume from the adsorption at $p/p_0 = 0.98$ and pore size distribution and mean pore size by the BDJH method applied to the desorption branch of the isotherm.

A Thermofinnigan TPDRO 1100 instrument was used for temperature-programmed reduction (TPR) experiments (10 °C/min with 5% H_2 in Ar, 25 mg of catalyst). Calibration was carried out using CuO; this allowed quantification of the TPR results and the estimation of the mean Mn oxidation state after assuming that at the end of the TPR experiments all Mn is e.g. as MnO.

Electron micrographs of the sample were taken on a HITACHI S-2700 scanning electronic microscope (voltage 15 kV). High resolution transmission electron microscopy (HRTEM) images were recorded using a JEOL-2010F, operated at 200 keV and with a spatial resolution at Scherzer defocus of 0.19 nm. High angle annular dark field-scanning transmission electron microscopy (HAADF-STEM) studies were performed on the same microscope with an electron probe of 0.5 nm of diameter at a diffraction camera length of 12 cm. This technique provides Z-contrast images that were used to determinate the platinum distribution on the support and its particle size distribution. Elemental analysis of the particles was performed by energy dispersive X-ray spectroscopy (EDXS, Oxford Inca Energy-200 detector). The samples were deposited by a dry method on commercial Cu grids coated by lacey-carbon.

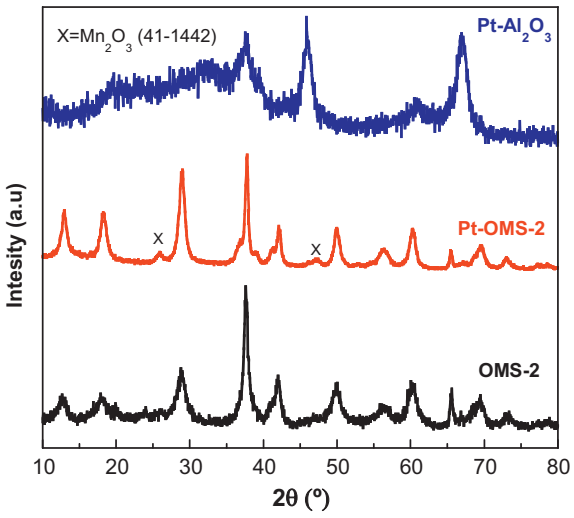

Fig. 1. X-ray diffraction pattern of the prepared catalyst.

The catalytic activity of the samples was evaluated by means of the ignition curves of toluene, ethyl acetate, their mixture (equicarbon atomic mixture), and MEK (methyl-ethyl-ketone) in air. Catalysts were pre-treated in air at 400 °C for 1 h prior to the reaction. Complete oxidation reactions were carried out in a tubular fixed-bed reactor at atmospheric pressure and heating rate of 2 °C/min. The ignition curves were obtained at 500 cm^3 min^{-1} of an air stream containing 1000 mg C Nm^{-3}. Conversion was obtained by measuring VOCs disappearance and the production of water by Mass Spectroscopy (Balzers Omnistar) or GC-TCD (HP 5890) together with CO_2 monitoring by an on-line detector (Vaisala GMT220). The yield to CO_2 was calculated as the ratio between the CO_2 concentration divided by its value measured when complete conversion at high temperature has been reached and no partial oxidation products were detected in significant amount during oxidation of toluene and ethyl acetate. In the case of MEK oxidation, the yields to the partial oxidation products were calculated as moles of MEK converted into a given product divided by the moles of MEK fed into the reactor.

3. Results

3.1. Catalyst characterization

3.1.1. XRD and nitrogen adsorption

The XRD patterns of OMS-2 and the Pt-OMS-2 catalyst are shown in Fig. 1. The main reflections of OMS-2 structure (JVPDS 29-1020) at 2θ angles of 12.8°, 18.5°, 37.5°, 42°, and 50° are present [17] and the peaks broadening is indicative of small crystal size. The XRD pattern showed no peaks corresponding to platinum, suggesting that the metal is highly dispersed on the support. In addition, two peaks corresponding to Mn_2O_3 were identified at 2θ angles around 26° and 46°. The XRD pattern of the Pt-Al_2O_3 catalyst showed the existence of the γ-alumina phase and no peaks corresponding to platinum (see Fig. 1).

Nitrogen adsorption–desorption isotherms and pore size distributions of the OMS-2 samples are shown in Fig. 2A. The isotherms recorded for these materials correspond to Type IV and the hysteresis loop is Type H1 for all materials, according to the IUPAC classifications suggesting the existence of cylindrical or constant cross-section pores. The pore size distributions show Gaussian

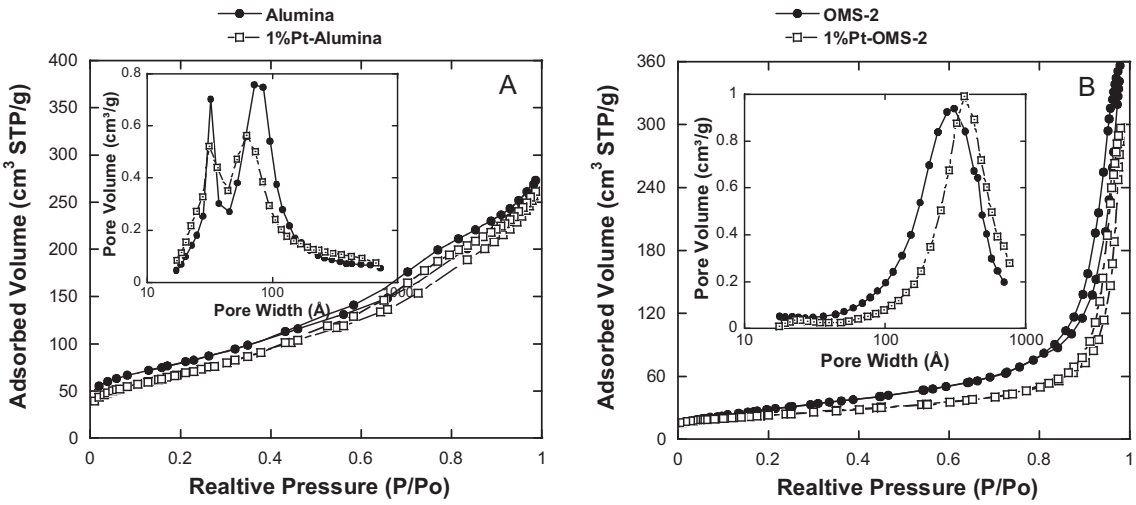

Fig. 2. Nitrogen adsorption–desorption isotherms and pore size distribution of the OMS-2 (A) and alumina samples (B).

Table 1
Textural properties of the indicated samples.

Catalyst	S_{BET} (m^2/g)	V_P (cm^3/g)
OMS-2	102	0.55
1% Pt-OMS-2	80	0.46
Al_2O_3	243	0.42
1% Pt-Al_2O_3	212	0.40

curves centered at 38 nm for OMS-2 and 30 nm for Pt-OMS-2. Table 1 summarizes the main textural parameters obtained from the nitrogen isotherms: BET surface area (S_{BET}) and total pore volume (V_P). Pt-OMS-2 shows surface area and pore volume approximately 20% lower than for the parent OMS-2. The specific surface area decreased slightly when Al_2O_3 is impregnated with Pt but the total pore volume did not change appreciably (see Table 1 and Fig. 2B).

3.1.2. SEM and TEM micrographs

Scanning electron microscopy (SEM) micrograph of OMS-2 (Fig. 3A) shows the characteristic acicular bunch morphology of this kind of Mn oxides. According to high resolution SEM and TEM images, the fibers exhibit diameters between 10 and 20 nm, being 15.4 nm the average diameter, whereas their aspect ratio is high (L/D = 10–20). HRTEM images show the details of the crystal structure, suggesting a preferential growth of the fibers along the [1 1 0] orientation. At the end of one fiber, it can be seen the 2×2 tunnel structure of OMS-2 (Fig. 3B inset). It should be pointed out that the OMS-2 morphology is unaffected by the platinum deposition process. Fig. 4A shows a typical STEM-HAADF image of the Pt-OMS-2 catalyst where the platinum particles can be distinguished as bright white contrasts due to the higher Z number of Pt in comparison with Mn. The platinum particle size distribution is included in Fig. 4B, being the calculated metal dispersion, 79%. Fig. 5A shows STEM-HAADF images of Pt-Al_2O_3, whereas Fig. 5B includes the Pt particle size distribution of this sample. The metal dispersion of the Pt-Al_2O_3 catalyst is 34%.

3.1.3. TPR profiles

Fig. 6 shows the H_2-TPR profiles of the OMS-2 and Pt-OMS-2 catalyst. For the OMS-2, the profile is featured by a main reduction peak at about 320 °C with a slight shoulder at the onset of the reduction (200 °C). The shoulder reduction peak is related to readily reducible small clusters of surface manganese oxides [18], and the intense peak represents the reduction of MnO_2 to MnO without formation of intermediate Mn_3O_4 [19]. The profile of Pt-OMS-2 exhibits two reduction peaks at around 150 and 400 °C. From the TPR results, the calculated average oxidation state of Mn decreases slightly from 3.93 in the OMS-2 to 3.83 in the Pt-OMS-2 catalyst.

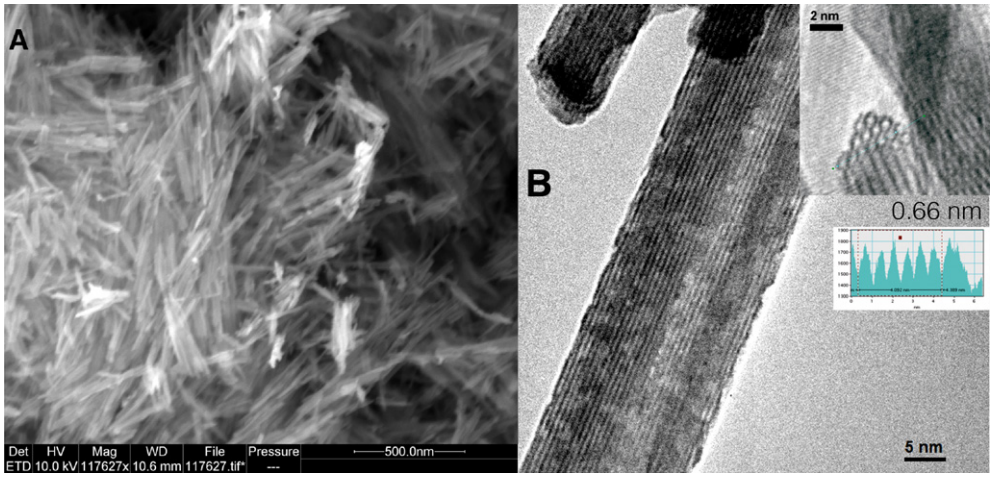

Fig. 3. SEM (A) and TEM (B) images of OMS-2.

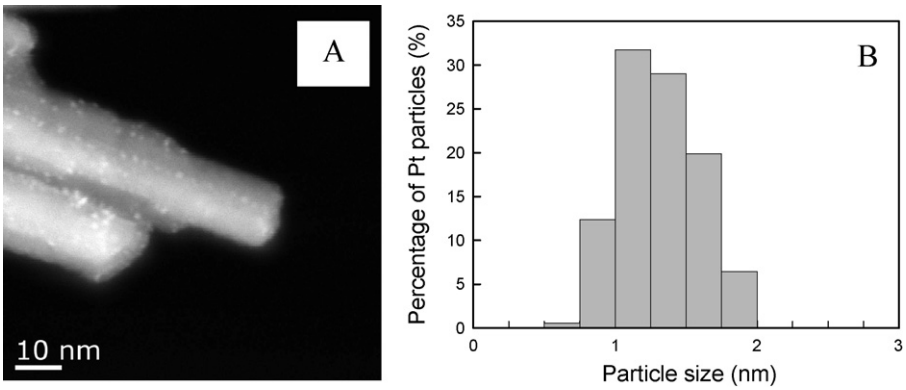

Fig. 4. STEM-HAADF images (A) and Pt particle size distribution (B) of Pt-OMS-2 catalyst.

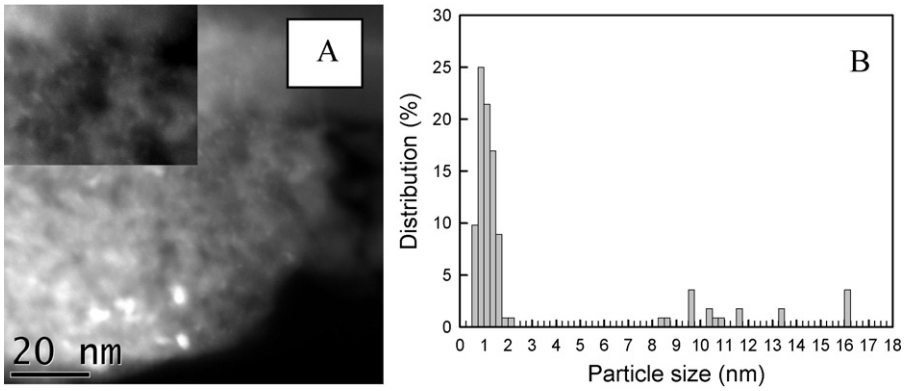

Fig. 5. STEM-HAADF images (A) and Pt particle size distribution (B) of Pt-Al_2O_3 catalyst.

3.2. Catalytic tests

3.2.1. Ethyl acetate, toluene and MEK combustion

The activity of the catalyst for the complete oxidation of the single VOCs is considered first. Regarding the oxidation of toluene and ethyl acetate (Fig. 7), tested catalysts did not produce significant amounts of intermediate oxidation products, yielding only CO_2 and H_2O. As a result, in these cases the ignition curves obtained through the signal corresponding to the disappearance of the VOC coincides with the ignition curve obtained from the signal of the CO_2 appearance.

From Fig. 7 it can be observed that Pt-OMS-2 is the most active combustion catalyst. Platinum improved the catalytic activity of OMS-2 decreasing the complete toluene oxidation temperature from 300 °C to 265 °C. On the other hand, on Pt-Al_2O_3 the combustion of toluene started at higher temperature than on Pt-OMS-2 although the temperature for complete oxidation was only 10 °C higher.

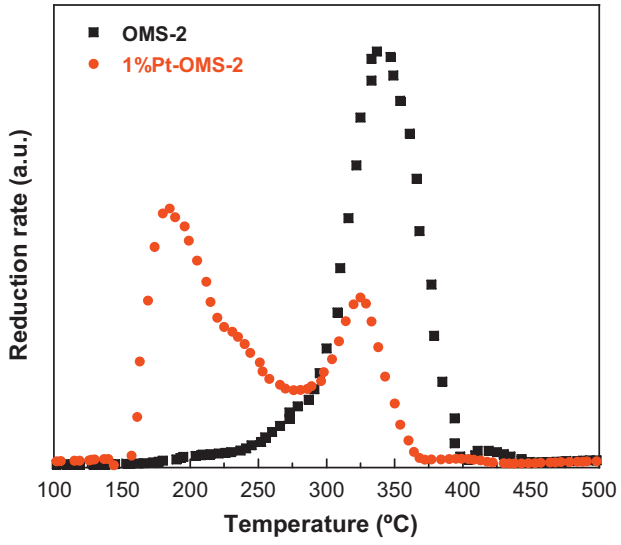

Fig. 6. TPR profiles of the OMS-2 catalysts.

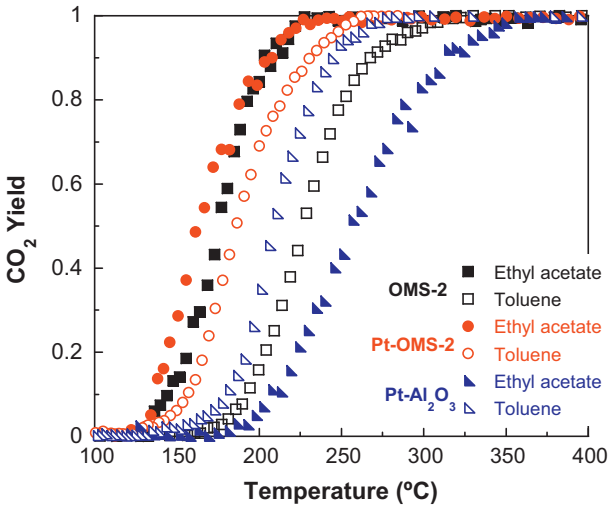

Fig. 7. Toluene and ethyl acetate ignition curves.

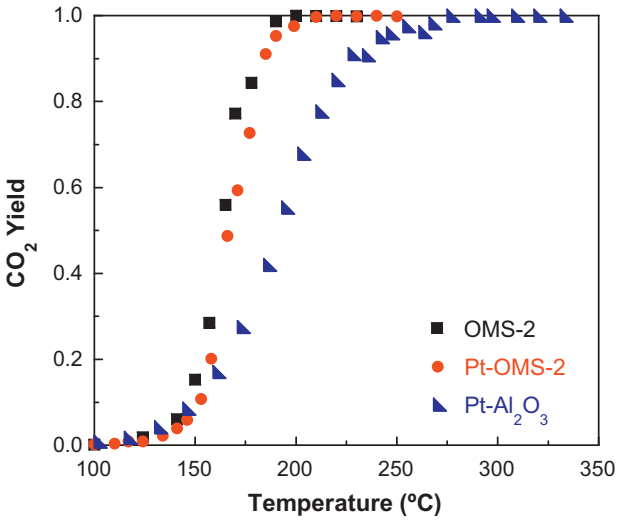

Fig. 8. MEK ignition curves.

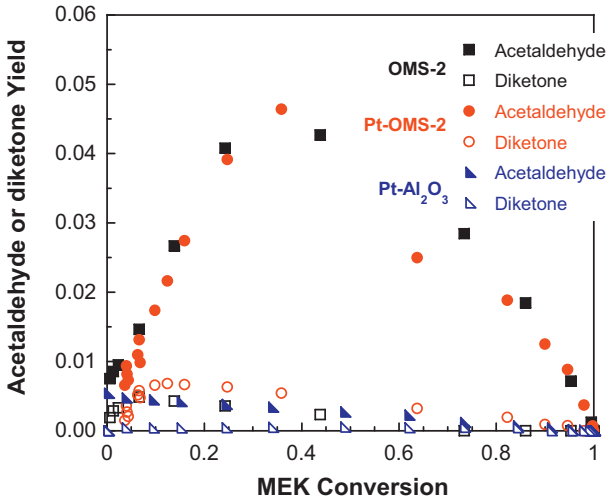

Fig. 10. Evolution of the partial oxidation products yield with MEK conversion.

As concerns the oxidation of ethyl acetate, cryptomelane-based samples (with and without platinum) showed very high and similar activities that allow oxidising completely this VOC at only 225 °C. The dispersion of platinum on the OMS-2 surface did not alter its activity to oxidise ethyl acetate. In contrast, with the Pt-Al_2O_3 catalyst it is necessary to attain 350 °C to obtain the total conversion.

The catalysts behaviour for MEK combustion is similar to that shown with ethyl acetate (see Fig. 8): there is no difference between the OMS-2 catalysts that achieve complete MEK conversion at 205 °C whereas Pt-Al_2O_3 needs a significantly higher temperature of 268 °C. It has been found that the values of the MEK conversion to CO_2 are lower than the total MEK conversion. This discrepancy stems from the fact that CO_2 and H_2O are not the only reaction products. In fact, the formation of partial oxidation products of MEK, namely acetaldehyde, methyl-vinyl-ketone and diketone has been detected. Figs. 9 and 10 show that the formation of partial oxidation products on Pt-Al_2O_3 is very low, that is, this catalyst presents higher selectivity to complete oxidation, while OMS-2, either with or without platinum, promotes the partial oxidation at intermediate conversion levels. Nevertheless, this does not represent any problem for using OMS-2 since at complete MEK conversion the only products are CO_2 and H_2O.

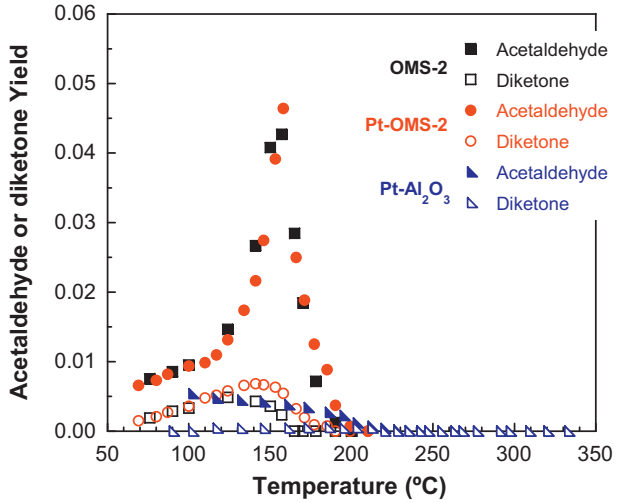

Fig. 9. Evolution of the partial oxidation products yield with reaction temperature.

Acetaldehyde was the most abundant partial oxidation product. Figs. 9 and 10 show the production of this intermediate as a function of the reaction temperature and the MEK conversion, respectively. Despite being the most abundant intermediate, the acetaldehyde yield did not exceed 4% with both cryptomelanes, and 0.5% for Pt-Al_2O_3. Analysing the evolution of the acetaldehyde yield with MEK disappearance (Fig. 10), both cryptomelanes show the same behaviour, with the maximum yield being achieved at around 35% MEK conversion.

Methyl-vinyl-ketone has been also identified, but the product yields were extremely low, less than 0.1%. As concerns diketone (2,3-butanedione), Figs. 9 and 10 show that this product is more abundant over the OMS-2 catalysts with maximum yields of 0.7 and 0.5% for Pt-OMS-2 and OMS-2, respectively. The maximum yield of methyl-vinyl-ketone is reached at lower MEK conversions, around 20%, than the maximum yield of acetaldehyde.

3.2.2. *Ethyl acetate–toluene mixture combustion*

Let us consider now the effect of mixing two VOCs, toluene and ethyl acetate (equi-carbon atomic mixture) with the same total concentration (1000 mg C N m^{-3}) used with the individual VOCs. As can be seen in Fig. 11A, Pt-OMS-2 shows the highest activity towards the combustion of the VOCs mixture, achieving complete conversion to H_2O and CO_2 at 215 °C. However, at that temperature OMS-2 and Pt-Al_2O_3 give VOCs mixture conversions of 65 and 70%, respectively. The conversion curve over Pt-Al_2O_3 shows two zones. The first one ends at 210 °C and has the typical aspect of an ignition curve; the second zone shows an almost linear increase of the conversion with temperature until 330 °C.

Fig. 11B presents the conversion of every component of the mixture. The Pt-OMS-2 catalyst shows the best performance for the combustion of both toluene and ethyl acetate. Pt-Al_2O_3, on the other hand, shows high activity for toluene combustion in the mixture whereas ethyl acetate oxidation starts only when almost complete toluene conversion has been obtained at about 190 °C. This behaviour explains the shape of the global conversion curve over this catalyst (Fig. 11A). This is the least active catalyst for ethyl acetate combustion in the mixture. OMS-2 presents an intermediate behaviour: as shown previously for the single VOCs it is much more active for ethyl acetate than toluene combustion, as a matter of fact toluene combustion over this catalysts is limiting as it requires relatively high temperatures, close to 300 °C. It can be seen that the incorporation of platinum over OMS-2 is more advantageous when considering the treatment of VOCs mixtures.

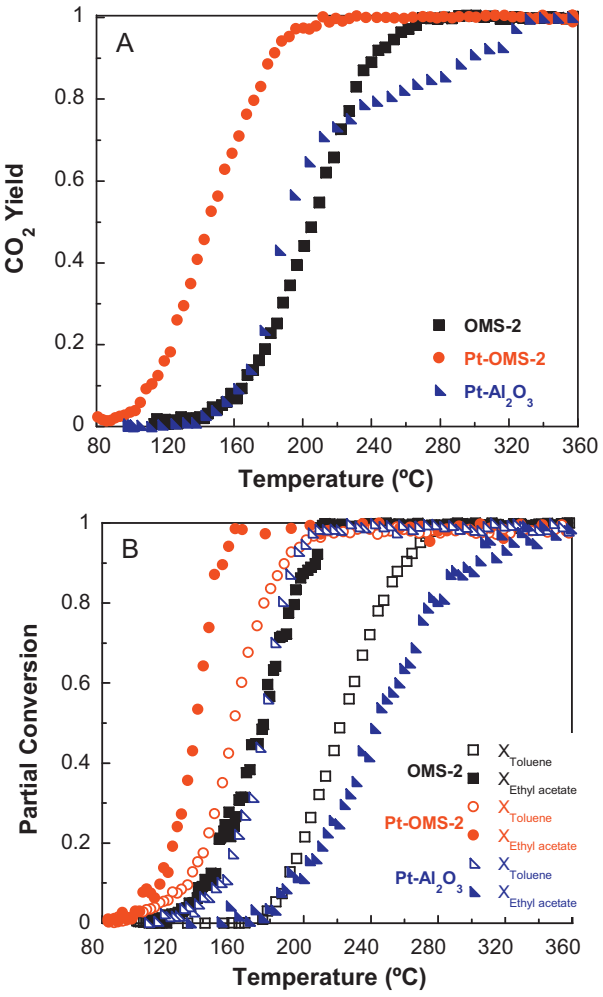

Fig. 11. Total conversion (A) and partial conversion of toluene and ethyl acetate in the VOCs mixture (B).

4. Discussion

In the present work platinum was supported on OMS-2 by wet impregnation. SEM images showed that the original needle-shaped nanocrystalline structure did not change after the impregnation with platinum (Fig. 3). XRD patterns indicate similar results (Fig. 1) showing that the OMS-2 structure is preserved after platinum incorporation. On other hand, the incorporation of platinum led to a moderate decrease of about 20% of the specific surface area and pore volume. Some α-Mn_2O_3 is present on Pt-OMS-2 as deduced from TPR and XRD results by the slight decrease of the Mn mean oxidation state and the diffraction peaks at 2θ angles around 26° and 46°. The TPR profile of the Pt-OMS-2 presents an H_2-consuption peak at much lower temperature than that of OMS-2 (Fig. 6). The peak around 190 °C is attributed to the reduction of PtOx and partial reduction of MnO_2 promoted by spillover of hydrogen species from Pt onto MnO_2 [11].

The VOCs removal is an important research topic in heterogeneous catalysis. Studies in this area should take into account not only the catalyst activity, selectivity or stability for the abatement of single VOCs of diverse chemical nature, but also the ability to oxidise simultaneously mixtures of VOCs. This study confirms results from previous work [15] showing that noble metals are not always more active than certain metal oxides. It has been found that some oxygenated VOCs such as ethyl acetate and MEK are comparatively more difficult to oxidise on Pt than on manganese oxide (OMS-2). For example, over Pt-Al_2O_3, which is a typical VOCs combustion catalyst, the oxidation of ethyl acetate alone occurs at temperatures that are up to 150 °C higher than on OMS-2 (see Fig. 7). In this case, the incorporation of Pt on OMS-2 does not improve the catalytic performance. Similarly for MEK combustion, another oxygenated VOC, 100% conversion is reached at 205 °C with OMS-2, while the Pt-Al_2O_3 catalyst gives a conversion of only 70% at the same temperature (see Fig. 8). In contrast, total conversion of toluene was obtained at 270 °C over Pt-Al_2O_3 whereas it was necessary to reach 300 °C over the OMS-2. It is widely accepted that the complete oxidation of VOCs over Pt starts with the breaking of the weakest C–H bond of the organic molecule. This is in accordance with the results of a previous study showing that the combustion of MEK over supported Pt catalyst takes place at lower temperatures than that of acetone [20]. A Langmuir–Hinshelwood–Hougen–Watson type kinetic model considering as limiting step the surface reaction between MEK and oxygen adsorbed on the same type of centers described reasonably well the reaction kinetics on Pt-Al_2O_3 [21]. However, in the case of metal oxides, and because of their acid–base properties [22], there is the possibility that carbonyl compounds as MEK or ethyl acetate interact with the catalyst via its enolic form, opening the possibility of new reaction routes as it is the case of the Mars-van Krevelen oxidation mechanism [23].

Toluene oxidation gives completely different results. In this case, the incorporation of Pt to OMS-2 improves the catalytic activity since it allows reducing the temperature for complete oxidation from 300 °C over OMS-2 to 265 °C over Pt-OMS-2 (Fig. 7). Therefore, it seems that for aromatic VOCs the presence of platinum improves the catalytic activity. There is the possibility that the combustion of toluene takes place preferentially on platinum whereas that of ethyl acetate and MEK on manganese oxide. Carnö et al. [24] studying mixed manganese oxide/platinum catalysts observed a different catalytic behaviour depending on the organic molecules properties. Naphthalene and CO conversion was favoured by the presence of platinum whereas methane oxidation was not affected. Wang et al. [11] observed that the activity for formaldehyde combustion increased after doping OMS-2 with platinum.

The combustion of MEK produced acetaldehyde and diketone as the main partial oxidation products as well as traces of methyl-vinyl-ketone. The yield of partial oxidation products was higher in the presence of OMS-2, with or without Pt, whereas Pt-Al_2O_3 was very selective to the complete oxidation products (Figs. 9 and 10). The evolution of the yields of acetaldehyde and diketone with the conversion of MEK over both OMS-2 and Pt-OMS-2 shows an increase with reaction temperature to reach a maximum value near the ignition point (35–40% MEK conversion), and then a continuous decrease to become zero at higher temperatures when 100% selectivity to CO_2 is reached. The capacity of interaction of ketones on manganese oxides could explain the formation of MEK partial oxidation products. In fact, the products detected in this work have also been found in studies on selective oxidation of MEK catalysed by V_2O_5-P_2O_5. It has been suggested that the interaction via the enolic form of the MEK gives rise to the products of partial oxidation [23]. Regarding the combustion of MEK over supported Pt catalysts, 100% selectivity to the complete oxidation products was found in previous works [21,21]. However, Arzamendi et al. [25] observed when using Pd-Mn/Al_2O_3 catalysts, acetaldehyde, methyl-vinyl-ketone, diketone and trace amounts of acetic acid during MEK combustion.

It is difficult to make a reliable comparison between the different catalysts that have been evaluated for ethyl acetate, MEK and toluene oxidation so far, as they have been tested under rather different experimental conditions, especially regarding to the concentration of VOCs and the space velocities employed.

In practice, a VOCs-containing waste stream is expected to consist of a rather complicated mixture of VOCs. Therefore, it is of

interest to see if it is possible to predict the performance of the catalyst under these conditions based on data concerning the oxidation of each component separately or of simple mixtures. In this work, the oxidation of a toluene–ethyl acetate mixture was studied. As far as metal oxides are concerned, the existing literature [15,26,27] indicate that interferences occurring when various VOCs are simultaneously oxidised may be understood in terms of competitive adsorption: the component which is preferentially adsorbed is oxidised first. The competition and interference between reactants result in an increase of the temperature at which complete removal of each VOC is achieved [15,27–30]. This behaviour is observed in the case of the Pt-Al_2O_3 catalyst: ethyl acetate elimination started after 100% conversion of toluene was obtained (Fig. 11B). With this catalyst, oxygenated compounds such us ethyl acetate are difficult to remove. The more strongly adsorbed VOC is no longer the easiest to oxidise. Lahousse et al. [15] observed for VOCs mixture combustion on Pt-TiO_2 that the most difficult to oxide compound very often controls the overall reaction, and that complete conversion of all components is achieved at temperatures, which are higher than that measured with the compound alone. In our case, when platinum was dispersed on OMS-2, the activity of the catalyst is higher than on bare OMS-2 and the competitive effects found on Pt-Al_2O_3 were not present, perhaps because toluene combustion can be performed on Pt and that of ethyl acetate simultaneously on the manganese oxide surface. In the absence of Pt, toluene combustion becomes limiting whereas in the absence of OMS-2 the limiting VOC is ethtyl acetate. In Pt-OMS-2 active sites for the oxidation of aromatic and oxygenated VOCs coexist which makes this catalyst very attractive to treat VOCs mixtures.

5. Conclusions

OMS-2 is an interesting support for Pt because high metallic dispersions can be achieved by simple incipient wetness impregnation while maintaining good textural properties as well as the OMS-2 structure of the manganese oxide. The incorporation of platinum onto the OMS-2 surface improves the performance of OMS-2 catalyst for the oxidation of toluene, but not the oxidation of MEK and ethyl acetate that remains unaffected.

The prepared Pt-OMS-2 catalyst is very active for the combustion of a toluene–ethyl acetate mixture. It appears that on this catalyst coexist sites as metallic platinum that catalyse the oxidation of toluene and sites on the manganese oxide surface where ethyl acetate occurs preferentially as deduced from the single VOC experiments. Therefore, the competitive effects found on the bare OMS-2 and especially Pt-Al_2O_3 were not present on Pt-OMS-2.

Acknowledgments

Financial support by the UPV/EHU (GIU07/63 and the “Ayuda de especialización de investigadores doctores en la UPV/EHU” to O.S.) and the Spanish Ministry of Science and Innovation (ENE2009-14522-C05 and Juan de la Cierva contract for P. Navarro) is gratefully appreciated.

References

[1] R.N. Deguzman, Y.-F. Shen, E.J. Neth, S.L. Suib, C.-L. ÒYoung, S. Levine, J. Newsam, Chem. Mater. 6 (1994) 815.
[2] D. Frías, S. Nousir, I. Barrio, M. Montes, T. López, M.A. Centeno, J.A. Odriozola, Mater. Charact. 58 (2007) 776.
[3] M.I. Domínguez, P. Navarro, F. Romero-Sarria, D.M. Frias, S.A. Cruz, J.J. Delgado, M.A. Centeno, M. Montes, J.A. Odriozola, J. Nanosci. Nanotechnol. 8 (2008) 1.
[4] D.M Frias, S. Nousir, I. Barrio, M. Montes, L.M. Martinez, M.A. Centeno, J.A. Odriozola, Appl. Catal. A 325 (2007) 205.
[5] R. Jothiramaligam, B. Viswanathan, T.K. Varadarajan, Catal. Commun. 6 (2005) 41.
[6] M.A. Wolfovichm, R. Jothuramalingam, M.V. Landau, M. Herskowitz, B. Viswanathan, T.K. Varadarajan, Appl. Catal. B 59 (2005) 91.
[7] X. Chen, Y.F. Shen, S.L. Suib, C.L. ÓYoung, J. Catal. 197 (2001) 292.
[8] R. Jothiramaligam, B. Viswanathan, T.K. Varadarajan, J. Mol. Catal. A 252 (2006) 49.
[9] H. Nur, F. Hayati, H. Hamdan, Catal. Commun. 8 (2007) 2007.
[10] R. Jothiramaligam, B. Viswanathan, T.K. Varadarajan, Mater. Chem. Phys. 100 (2006) 257.
[11] R. Wang, J. Li, Catal. Lett. 131 (2009) 500.
[12] W. Gac, Appl. Catal. B 75 (2007) 107.
[13] X. Chen, Y.F. Shen, S.l. Suib, C.L. ÓYoung, Chem. Mater. 14 (2002) 940.
[14] N. Watanabe, H. Yamashita, H. Miyadera, S. Tominga, Appl. Catal. B 8 (1996) 405.
[15] C. Lahousse, A. Bernier, P. Grange, B. Delmon, P. Papaefthimiou, T. Ioannides, X.E. Verykios, J. Catal. 178 (1998) 214.
[16] J. Luo, Q. Zhang, A. Huang, S.L. Suib, Microporous Mesoporous Mater. 35 (2000) 209.
[17] M.A. Cheney, N.R. Birkener, L. Ma, T. Hartmann, P.K. Bhowmik, V.F. Hodgeb, S.M. Steinberg, Colloids Surf. A: Physicochem. Eng. Aspects 289 (2007) 185.
[18] X.F. Tang, J.L. Chen, X.M. Huang, Y.D. Xu, W.J. Shen, Appl. Catal. B 81 (2008) 115.
[19] R. Xu, X. Wang, D.S. Wang, K.B. Zhou, Y.D. Li, J. Catal. 237 (2006) 426.
[20] A. Gil, M.A. Vicente, J.-F. Lambert, L.M. Gandía, Catal. Today 68 (2001) 41.
[21] G. Arzamendi, R. Ferrero, A.R. Pierna, L.M. Gandía, Ind. Eng. Chem. Res. 46 (2007) 9037.
[22] G. Busca, E. Finocchio, G. Ramis, G. Ricchiardi, Catal. Today 32 (1996) 133.
[23] E. McCullagh, J.B. McMonagle, B.K. Hodnett, Appl. Catal. A 93 (1993) 203.
[24] J. Carnö, M. Ferrendon, E. Björnbom, S. Järas, Appl. Catal. A 155 (1997) 265.
[25] G. Arzamendi, V.A. de la Peña O'Shea, M.C. Álvarez-Galván, J.L.G. Fierro, P.L. Arias, L.M. Gandía, J. Catal. 261 (2009) 50.
[26] J.J. Spivey, Ind. Eng. Chem. Res. 26 (1987) 2165.
[27] S.M. Saqer, D.I. Kondarides, X.E. Verykios, Appl. Catal. B 103 (2011) 275.
[28] P. Papaefthimiou, T. Ioannides, X.E. Verykios, Appl. Catal. B 5 (1998) 75.
[29] P. Papaefthimiou, T. Ioannides, X.E. Verykios, Appl. Catal. B 13 (1997) 175.
[30] V. Blasin-Aubé, J. Belkouch, L. Monceaux, Appl. Catal. B 43 (2003) 175.